

The shape of the velocity ellipsoid in NGC 488

Joris Gerssen¹, Konrad Kuijken¹ and Michael R. Merrifield²

¹*Kapteyn Institute, Groningen 9700 AV, The Netherlands*

²*Department of Physics and Astronomy, University of Southampton, Highfield, SO17 1BJ.*

1 October 2018

ABSTRACT

Theories of stellar orbit diffusion in disk galaxies predict different rates of increase of the velocity dispersions parallel and perpendicular to the disk plane, and it is therefore of interest to measure the different velocity dispersion components in galactic disks of different types. We show that it is possible to extract the three components of the velocity ellipsoid in an intermediate-inclination disk galaxy from measured line-of-sight velocity dispersions on the major and minor axes. On applying the method to observations of the Sb galaxy NGC 488, we find evidence for a higher ratio of vertical to radial dispersion in NGC 488 than in the solar neighbourhood of the Milky Way (the only other place where this quantity has ever been measured). The difference is qualitatively consistent with the notion that spiral structure has been relatively less important in the dynamical evolution of the disk of NGC 488 than molecular clouds.

Key words: galaxies: fundamental parameters – galaxies: individual: NGC488 – galaxies: kinematics and dynamics.

1 INTRODUCTION

It is observationally well established that the velocity dispersion of main sequence stars increases with advancing spectral type. This fact has been recognised ever since velocity dispersions were first measured in the solar neighbourhood (e.g. King 1990). Initially these observations were explained as the result of equipartition of energy because the mass of the stars decreases along the main sequence. However the two-body relaxation time scale is much too long to have any effect on the stellar velocity ellipsoid, prompting explanations relying on collective effects instead. Some of the different functional forms that have been suggested for the velocity dispersion-age relation are reviewed by Lacey (1991). This increase in velocity dispersion, or heating, depends on the roughness of the gravitational potential in the disk, so knowledge about the shape of the velocity ellipsoid will tell us a great deal about the dynamical history of a disk.

Until recently direct measurements of the three-dimensional shape of the velocity ellipsoid have been restricted to the solar neighbourhood. Observations of the stellar velocities in external spiral galaxies have concentrated on systems that are either close to edge-on or face-on (van der Kruit and Freeman 1986; Bottenga 1995) and will therefore only provide information about a single component of the velocity dispersion. From these measurements only indirect inferences can be drawn about the shape of velocity ellipsoids in galaxies because the results of a small sample of *different* galaxies are being compared in a statistical

way. Moreover, this shape will be subject to rather large uncertainties because the errors of the face-on and edge-on galaxies are compounded, and because relating face-on and edge-on galaxies is rather delicate.

In this pilot study we show that it is possible to derive the shape of the velocity ellipsoid within a *single* galaxy. We use the fact that an intermediate-inclination galaxy shows different projections of the velocity dispersion at different galactocentric azimuths. In section 2 the method by which we extract the velocity dispersions information is described. In section 3 we apply this analysis to the large early type spiral NGC 488 and in section 4 we discuss the results obtained for NGC 488 and compare them to the velocity ellipsoid in the solar neighbourhood.

2 ANALYSIS

In cylindrical polar coordinates (R, ϕ, z) the line-of-sight velocity dispersion as a function of (intrinsic) position angle ϕ in a thin axisymmetric disk is

$$[\sigma_R^2 \sin^2 \phi + \sigma_\phi^2 \cos^2 \phi] \sin^2 i + \sigma_z^2 \cos^2 i, \quad (1)$$

which can be written as

$$\frac{1}{2} \sin^2 i [(\sigma_R^2 + \sigma_\phi^2 + 2\sigma_z^2 \cot^2 i) - (\sigma_R^2 - \sigma_\phi^2) \cos 2\phi]. \quad (2)$$

Thus, it consists of an element with a $\cos 2\phi$ variation that depends only on the components of the dispersion in the plane of the galaxy, and an element with no dependence

on ϕ that depends on all three components of the velocity dispersion. Observations along at least two axes (preferably the major and minor axes, which provide maximum leverage), are therefore required to extract both coefficients. Furthermore, in disk galaxies, in which most orbits are well-described by the epicycle approximation the radial and azimuthal dispersions obey the relation

$$\frac{\sigma_\phi^2}{\sigma_R^2} = \frac{1}{2} \left(1 + \frac{\partial \ln V_c}{\partial \ln R} \right), \quad (3)$$

where V_c is the circular speed in the galaxy. (In the solar neighbourhood, this expression reduces to $-B/(A-B)$, where A and B are the Oort constants.) Within the epicycle approximation the stellar rotation speed $\bar{V}(R)$ equals the circular speed $\sqrt{R\partial\Psi/\partial R}$, so the righthand side of eq. 3 can be derived from the same spectral observations that are used to measure the velocity dispersions. The effect of higher-order approximations on this formula are discussed by Kuijken & Tremaine 1991, who showed that the strongest deviations from eq. 3 are to be found at radii of several disk scale lengths (see also Cuddeford & Binney 1994).

Where the circular speed V_c can be measured separately (e.g., from an emission-line rotation curve), a further constraint on the dispersions and velocities is the asymmetric drift equation,

$$V_c^2 - \bar{V}^2 = \sigma_R^2 \left[\frac{R}{h} - R \frac{\partial}{\partial R} \ln(\sigma_R^2) - \frac{1}{2} + \frac{R}{2V_c} \frac{\partial V_c}{\partial R} \right] - R \frac{\partial \sigma_{Rz}^2}{\partial z} \quad (4)$$

The last term of equation 4 describes the tilting of the velocity ellipsoid. The two limiting cases of this tilting term are zero and $(\sigma_R^2 - \sigma_z^2)$. Orbit integration by Binney & Spergel (1983) and by Kuijken & Gilmore (1989) suggest that in the solar neighbourhood the truth lies close to midway between the two extremes. As will be seen below, the uncertainty in this term is not a concern in the present analysis.

In summary, the three components of the stellar velocity ellipsoid can be deduced from measurements of the line-of-sight dispersions along two position angles in a galaxy disk. The two sets of measurements, together with the ratio of tangential and radial velocity dispersions appropriate for nearly circular orbits, provide the three equations necessary to deproject the ellipsoid. If the asymmetric drift can also be measured, e.g. when a rotation curve for cold interstellar gas is available, the system is overdetermined, allowing a consistency check on the result.

3 NGC 488

We choose the large early type spiral NGC 488 for this analysis because of its regular optical appearance and its intermediate inclination. Table 1 lists some properties of this galaxy. Note the very high rotational velocity (Peterson 1980).

B and I band images of NGC 488 were obtained with the 48 inch telescope at Mt. Hopkins observatory in September 1992. Bulge-disk decompositions were performed on these images to assess the extent to which the bulge contaminated the velocity dispersions of the disk. The light profiles obtained from these images along the major and minor axis are textbook examples of an exponential disk and a $R^{1/4}$ bulge, see fig. 1. After subtracting a straight line fit to the

Table 1. Parameters of NGC 488

Hubble type	Sb
Inclination	40°
Distance	30 Mpc (for H_0 of 75)
Max. rotational velocity	360 km/s
Angular size	5.2 x 3.9 arcmin
Photometric scale length	40" in B

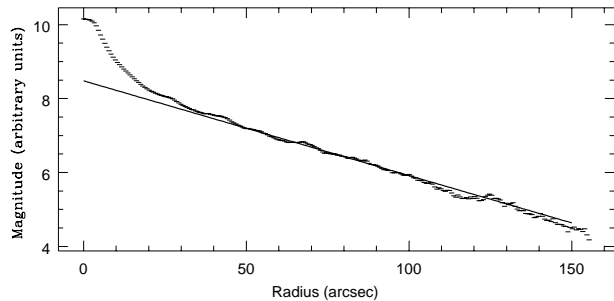


Figure 1. Major-axis I-band light profile of NGC 488. The line shows an exponential fit to the disk luminosity.

linear part of light profile we found that beyond a radius of 20 arcsec the disk-to-bulge light ratio increases rapidly. At 20 arcsec this ratio is about 7 and at 30 arcsec it is already 25. Data points at radii smaller than 20 arcsec were therefore excluded from the analysis. The derived scale lengths (~ 40 arcsec along the B band major axis) are in good agreement with the literature values (e.g. Shombert & Bothun 1987). The ratio of the minor to major axis scale lengths implies an inclination of $41^\circ \pm 6^\circ$, again in good agreement with the literature value of 40° . The scale lengths of the I band image are approximately 20% shorter than the B band scale lengths. This effect is usually attributed to obscuration by dust, but de Jong (1995) finds that such colour gradients are best explained by differences in the star formation history as a function of radius.

3.1 Stellar absorption line data

Two longslit spectra of NGC 488 were obtained with the Multiple Mirror Telescope in January 1994 using the Red Channel Spectrograph: a 3 hour integration spectrum along the major axis and a 2 hour integration along the minor axis. Both spectra were centered around the Mg b triplet at 5200Å. Calibrating arc lamp exposures were taken every 30 minutes. The dispersion per pixel is $\sim 0.7\text{Å}$.

The longslit spectra were reduced to log-wavelength bins in the standard way, using IRAF packages. Adjacent spectra were averaged to obtain a signal-to-noise ratio of at least 25 per bin, and the absorption-line profiles of these co-added spectra were analysed.

Analysis of the absorption line profiles using the algorithms of Kuijken & Merrifield (1993) and van der Marel & Franx (1993) revealed no significant departures from a gaussian distribution in the stellar velocity distributions, so all velocity dispersions were derived by the traditional gauss-

Table 2. Best-fitting parameters for the model distributions. The quoted errors are one sigma errors.

Parameter	fit 1	fit 2
V_{40} (km/s)	336 ± 8	327 ± 5
α	0.21 ± 0.04	0.27 ± 0.04
$\sigma_{R,0}$ (km/s)	253 ± 32	237 ± 38
$\sigma_{z,0}$ (km/s)	164 ± 27	176 ± 30
a (arcsec)	38 ± 4	38 ± 4
σ_z/σ_R	0.65 ± 0.16	0.74 ± 0.22

fitting methods using a single template star (HD 2841, spectral type K5III) to spatially co-added spectra. We note that the models of Kuijken & Tremaine (1991), based on the Shu (1969) distribution function, predict small skewness for the distribution of azimuthal velocity distribution within 1 disk scale length; such a marginally non-gaussian shape would not affect our analysis significantly.

3.2 Analysis

We applied the analysis described in section 2 to the spectra. Due to the noise present in the data we could not obtain the three components of the velocity dispersion directly (Merrifield & Kuijken, 1994) and adopted therefore a model fitting-approach. We assumed the following models for the velocity dispersions:

$$\sigma_R = \sigma_{R,0} \exp(-R/a); \quad (5)$$

$$\sigma_z = \sigma_{z,0} \exp(-R/a). \quad (6)$$

We also assumed that the circular velocity could be described by a power-law $V_c = V_{40}(R/40'')^\alpha$ and used equation 4 to relate V_c to the stellar rotation speed.

These model distributions were fitted simultaneously to our observables σ_{minor} , σ_{major} and $\overline{V}(R)$ using the non linear fit routines described in Press et al. (1986).

The best-fit parameters that we obtained are shown in table 2. In fit 1 the tilting term in equation 4 is set to zero, while in fit 2 it set equal to the other extreme possible value, $\sigma_R^2 - \sigma_z^2$. Both fit the data equally well. The χ^2 value of fit 1 is only marginally better than that of fit 2, and so these data cannot distinguish between the two extreme models for the tilting term. It is, however, interesting to note that sufficiently accurate data might allow the tilting term to be measured by such a comparison, perhaps providing constraints on the shape of the potential close to the disk. The error in the derived axis ratio of the velocity ellipsoid is slightly larger than one would naively expect because σ_R and σ_z are anti-correlated. Adopting the average between fits 1 and 2 as representing the most realistic tilting term, we obtain

$$\frac{\sigma_z}{\sigma_R} = 0.70 \pm 0.19. \quad (7)$$

We have tested this procedure on a large (~ 500) set of artificial major and minor axis spectra, created from the template star to resemble the observed galactic spectra as closely as possible, with a different poisson noise realisation for each spectrum. The best-fit parameters obtained from these spectra scatter with the same dispersion as the errors

obtained from any individual fit to a spectrum. Therefore, we conclude that the parameters returned by the fit programme are reliable.

An obvious extension to our fitting procedure would be to use different scale lengths for the R and z dispersion components. Unfortunately the data are not of sufficient quality to allow for a six parameter fit. One of the six eigenvalues that we obtained from diagonalising the correlation matrix was much larger than the other five, a clear indication that a six parameter fit is stretching the data a bit too much.

Interestingly, the kinematic scale length of the disk appears to be comparable to the photometric one. This is not the expectation from local isothermal approximation for disks, which predicts a scale length double the photometric one. The most likely explanation is probably the fact that we measure the scale length in the B band while the stellar mass distribution is best traced in the K band, the near infra-red. Empirically it is found that scale lengths in the K band are shorter than the B band up to a factor of about 2 (de Jong 1995, figure 4 and Peletier et al. 1996). Alternatively the approximation of a local isothermal distribution breaks down.

3.3 The emission line data

The fits described above are to the stellar data only. The lowest panel in fig. 2 shows the emission line data of Peterson and the predictions from our two fits. Both our fits are fully consistent with these data, and provide extra confirmation of the validity of our analysis. (A simple power-law fit to the emission-line data plotted in fig. 2 gives a power index of 0.18 ± 0.13 .) Unfortunately there are no measured emission line velocities in the inner part of the disk. Peterson gives velocities around 195 km/s near a radius of 10 arcsec which are a little higher than our fits would predict. However there is no reason why a power-law rotation curve should persist into those central, bulge dominated regions.

4 DISCUSSION

This is the first direct measurement of the vertical-to-radial velocity dispersion ratio anywhere outside the solar neighbourhood. Previous determinations have all been indirect, and hence suffer from large uncertainties. The method we have described here is quite straightforward, and could be applied to many systems.

The derived value of 0.70 ± 0.19 , which is effectively the average ratio near one photometric scale length, is somewhat higher than the solar neighbourhood value of 0.52 ± 0.03 that Wielen (1977) derived from the McCormick sample of K and M dwarfs. However, the error of 0.03 is the purely statistical error, but the scatter between the published observational estimates of this ratio suggests that the true error may be larger (see Lacey 1991).

Any difference between the two ratios is consistent with the findings about the relative effects of the two dominant heating mechanisms, molecular clouds and spiral structure, as we now show.

Heating by molecular clouds was originally proposed by Spitzer and Schwarzschild (1951). They proposed that stars in star-cloud encounters gain kinetic energy at the expense

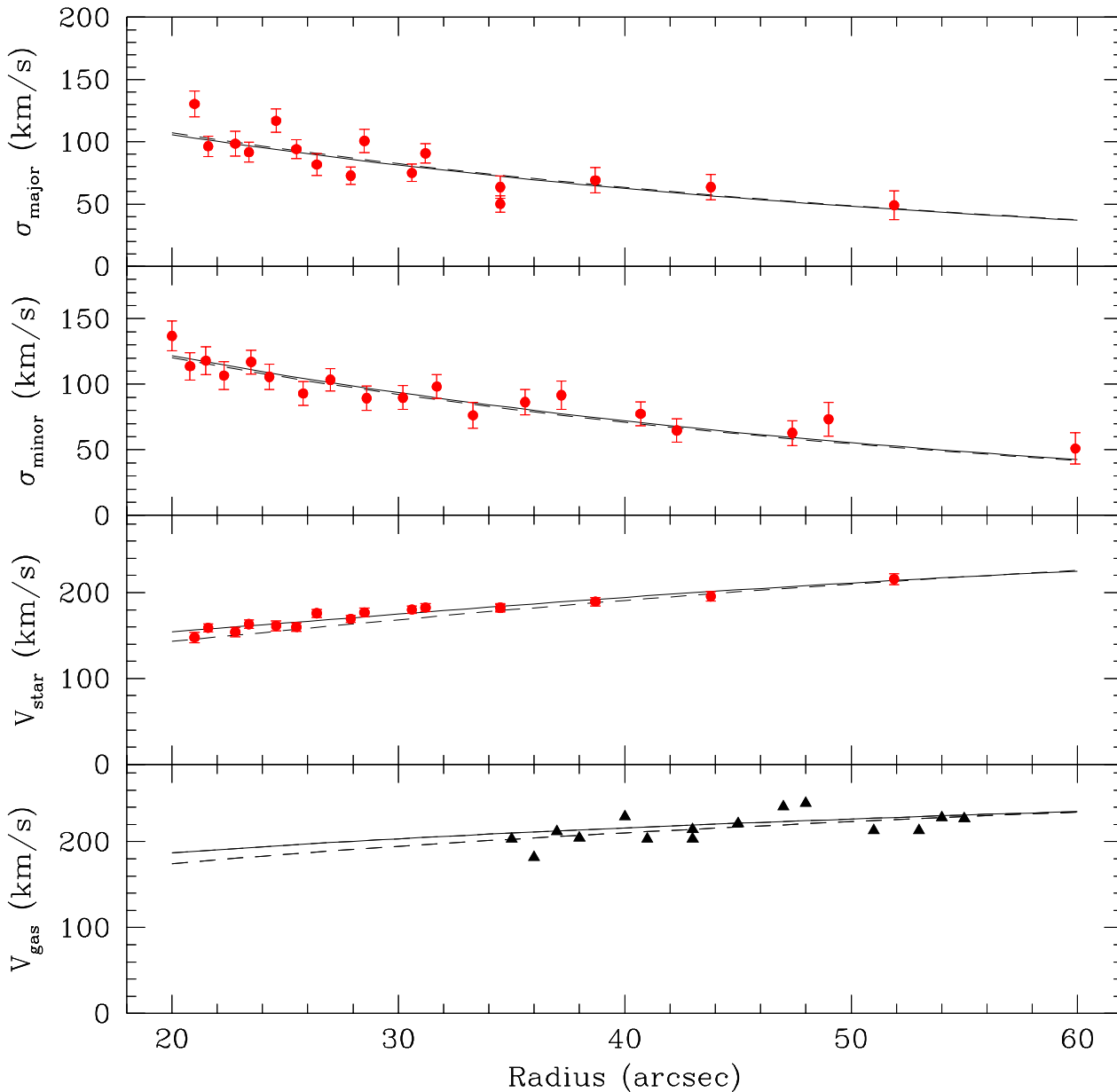


Figure 2. The best-fitting model distributions (solid line is fit 1 and the dashed line is fit 2) and the data. At radii smaller than 20 arcsec the bulge contaminates the disk light so data within that region were not included in the fit. The triangles in the lowest panel are the emission-line data of Peterson (1980).

of the clouds because of the huge masses of the latter. Subsequent analysis by Lacey (1984) and n -body simulations by Villumsen (1985) showed however that this mechanism saturates rather quickly (once the stars have sufficient energy that they spend most of their time outside the cloud layer the heating rate drops) and could not fully explain the observed heating.

An alternative proposal to heat the disk, due to Barbanis and Woltjer (1967), explains the heating as the result of stars scattering from spiral irregularities in the galactic potential. Carlberg and Sellwood (1985) have extended this

work and showed that this can indeed heat up the disk. However this process cannot heat the stars efficiently in the vertical direction because the vertical oscillation frequency of stars is much larger than the frequency at which a spiral wave sweeps past the stars orbiting the disk. Hence the stars respond almost adiabatically to this force.

Giant molecular clouds create large spiral wakes, often much larger than a cloud itself (Julian and Toomre 1966). This interplay between clouds and spiral irregularities is not yet completely understood but it is clear that they are not independent. Jenkins and Binney (1990) examined the com-

bined effects of both processes based on Monte Carlo simulations of the Fokker-Planck equation describing these processes. They expressed the relative importance of heating by spiral structure to heating by clouds by a parameter denoted β and calculated the corresponding ratio of σ_z/σ_R (see their figure 2). From the observed shape of the velocity ellipsoid and velocity dispersion-age relations they concluded that in the solar neighbourhood the heating of the disk is dominated by spiral structure ($\beta \sim 90$).

The mean surface density of the cloud layer near the sun is $1.8 M_\odot \text{ pc}^{-2}$ (Clemens, Sanders and Scoville 1988). From the FCRAO extragalactic CO survey (Young et al. 1995) a mean surface density for NGC 488 is derived of $3.5 M_\odot \text{ pc}^{-2}$. (Young et al. find that the CO layer in NGC 488 is best described by a uniform distribution with a radius of 1.65 arcmin and a CO flux of $S_{\text{CO}} = 540 \pm 130 \text{ Jy km/s.}$), higher than in the solar neighbourhood. NGC 488 is classified as an Sb galaxy. It has a very regular tightly wound spiral pattern (the pitch angle is only 5°). It is therefore quite likely that the potential associated with this spiral pattern is much smoother than that of our own Galaxy, which has an Sbc Hubble type. Both these observations imply that the parameter β must be smaller for NGC 488 than for the solar neighbourhood. According to the predictions of Jenkins and Binney a smaller β corresponds to a larger σ_z/σ_R ratio.

We do indeed find that the σ_z/σ_R ratio for NGC 488 is higher than for the Milky Way, however the difference is only one sigma. We conclude therefore that the shape of the velocity ellipsoid that we have determined is qualitatively consistent with the picture sketched by Jenkins and Binney.

The technique we have described in this paper would be straightforward to apply to a larger sample of disk galaxies. With higher quality data, it would also be possible to extend the analysis to map out the radial variation of the velocity ellipsoid shape, a quantity which has never been observationally constrained. Both projects would provide important measurements for comparison with the theoretical treatments of the heating processes in stellar disks.

ACKNOWLEDGMENTS

The data presented in this paper were obtained using the Multiple Mirror Telescope, which is a joint facility of the Smithsonian Institute and the University of Arizona. Much of the analysis was performed using IRAF, which is distributed by NOAO. We thank the referee, Cedric Lacey for his helpful comments.

REFERENCES

- Barbanis B., Woltjer L., 1967, ApJ, 150, 461
 Binney J., Spergel D. N., 1983, IAU Colloquium No. 76
 Bottema R., 1995 *PhD thesis, University of Groningen*
 Carlberg R. G., Sellwood J. A., 1985, ApJ, 292, 79
 Clemens D. P., Sanders D. B., Scoville N. Z., 1988 ApJ, 327, 139
 Cuddeford P., Binney J., 1994, MNRAS, 266, 273
 de Jong R. S., 1995 *PhD thesis, University of Groningen*
 de Jong R. S., 1996, A&A, 313, 45
 Jenkins A., Binney J., 1990, MNRAS, 245, 305
 Julian W. H., Toomre A., 1966, ApJ, 146, 810

- King I. R., 1990, in *The Milky Way as a Galaxy*, eds Buser R., King I. R., p. 172
 Kuijken K., Gilmore, G., 1989, MNRAS, 239, 571
 Kuijken K., Tremaine S., 1991 in *Dynamics of Disc Galaxies*, ed. Sundelius B., p. 71
 Kuijken K., Merrifield M. R., 1993, MNRAS, 264, 712
 Lacey C. G., 1984, MNRAS, 208, 687
 Lacey C. G., 1991, in *Dynamics of Disc Galaxies*, ed. Sundelius B., p. 257
 Merrifield M., Kuijken K., 1994, ApJ, 432, 575
 Peletier R. F. et al., 1996 A&A, 300, L1
 Peterson C. J., 1980, AJ, 85, 226
 Press et al., 1986, *Numerical Recipes*, Cambridge University Press, Cambridge
 Shombert J. M., Bothun G. D., 1987, AJ, 93, 29
 Shu F. H., 1969, ApJ, 158, 505
 Spitzer L., Schwarzschild M., 1951, ApJ, 114, 385
 van der Kruit P. C., Freeman K., 1986, ApJ, 303, 556
 van der Marel R. P., Franx M., 1993, ApJ, 407, 525
 Villumsen J. V., 1985, ApJ, 290, 75
 Wielen R., 1977, A&A, 60, 263
 Young J. S., et al., 1995, ApJSupl, 98, 257